J. Phys. D: Appl. Phys. **42** (2009) 175506 (7pp) doi:10.1088/0022-3727/42/17/175506

Determining the elastic modulus of thin films using a buckling-based method: computational study

Xiu-Peng Zheng[1], Yan-Ping Cao[1,4], Bo Li[1], Xi-Qiao Feng[1,4], Hanqing Jiang[2] and Yonggang Y Huang[3]

[1] AML, Department of Engineering Mechanics, Tsinghua University, Beijing 100084, People's Republic of China
[2] Department of Mechanical and Aerospace Engineering, Arizona State University, Tempe, AZ 85287, USA
[3] Department of Mechanical Engineering, Northwestern University, 2145 Sheridan Road, Evanston, IL 60208, USA

E-mail: caoyanping@tsinghua.edu.cn (Y P Cao) and fengxq@tsinghua.edu.cn (X Q Feng)

Received 14 June 2009, in final form 21 July 2009
Published 17 August 2009
Online at stacks.iop.org/JPhysD/42/175506

Abstract
The buckling mode of a thin film lying on a soft substrate has been used to determine the elastic modulus of thin films and one-dimensional objects (e.g. nanowires and nanotubes). In this paper, dimensional analysis and three-dimensional nonlinear finite element computations have been made to investigate the buckling of a film with finite width bonded to a compliant substrate. Our study demonstrates that the effect of Poisson's ratio of the film can be neglected when its width–thickness ratio is smaller than 20. For wider films, omitting the influence of Poisson's ratio may lead to a significant systematic error in the measurement of the Young's modulus and, therefore, the film should be treated as a plate. It is also found that the assumption of the uniform interfacial normal stress along the width of the film made in the theoretical analysis does not cause an evident error, even when its width is comparable to its thickness. Based on the computational results, we further present a simple expression to correlate the buckling wavelength with the width and thickness of the film and the material properties (Young's moduli and Poisson's ratios) of the film and substrate, which has a similar form to that in the classical plane-strain problem. The fundamental solutions reported here are not only very accurate in a broad range of geometric and material parameters but also convenient for practical use since they do not involve any complex calculation.

(Some figures in this article are in colour only in the electronic version)

1. Introduction

The buckling of a stiff layer on a compliant substrate was addressed a long time ago in the context of structural sandwich panels [1], and it remains a critical and fundamental issue in mechanics of materials. Recently, considerable efforts have been directed towards understanding the physical mechanisms underlying various phenomena associated with surface buckling and generating controlled buckling patterns on different length scales, which involve various applications in such fields as thin-film metrology [2–7], stretchable electronics [8–10] and optical gratings [11]. This study is concerned with the application of the buckling mode of a relatively stiff layer on a compliant substrate to measure the elastic modulus of the former. Cerda and Mahadevan [12] pointed out that research on the geometry and physics of wrinkling could form the basis of a highly sensitive quantitative wrinkling assay for the mechanical characterization of thin solid membranes. Stafford *et al* [2] proposed a buckling-based technique to measure the moduli of ultra-thin polymeric films. It uses the

[4] Authors to whom any correspondence should be addressed.

following fundamental relation to correlate the wavelength, film thickness and material properties in the plane-strain case [13–15]:

$$\lambda_0 = 2\pi h \left(\frac{E_f^*}{3E_s^*}\right)^{1/3}, \tag{1}$$

where λ_0 is the wavelength and h the thickness of the film. $E^* = E/(1-\nu^2)$ is the plane-strain modulus and ν the Poisson's ratio. Throughout this paper, the subscripts 'f' and 's' stand for the film and the substrate, respectively.

Recently, the buckling-based technique proposed by Stafford *et al* [2] has been demonstrated to be applicable in a wide range of problems by using different fundamental relations. For example, Huang *et al* [7] developed a new relation to determine the Young's modulus of an ultra-thin film when the effects of surface stresses are significant. Khang *et al* [16] measured the wavelength of buckled single-walled carbon nanotubes on a PDMS substrate to calculate the elastic modulus of the former. It is noted that equation (1) is based on the infinitesimal strain assumption, and when the substrate undergoes finite deformation, the result reported by Jiang *et al* [17] and Song *et al* [18] should be used to measure the Young's moduli of the film. The application of equation (1) also requires that the width of the film is much larger than its buckling wavelength. Or specifically, equation (1) is for plane-strain problems. In many practical measurements, however, this condition may not be satisfied. For instance, when the technique is applied to a stretchable metal interconnect [8–10], which is a one-dimensional-like stripe, the plane-strain assumption seems to be improper and equation (1) may lead to significant errors. In this case, Tarasovs and Andersons [19] and Jiang *et al* [20] investigated, both numerically and theoretically, the buckling of a film with a finite width lying on a compliant substrate. Their studies indicate that for relatively narrow films, the wavelength predicted by equation (1) can be much larger than the actual value. The analyses of Tarasovs and Andersons [19] and Jiang *et al* [20] help understand the effects of the finite width of the film and are valuable for practical measurements. However, it is still of paramount interest to further investigate the fundamental relations used in the buckling-based technique for measuring the elastic modulus of thin films. For instance, the film has been treated as a beam in the previous theoretical studies and thus the effect of its Poisson's ratio has not been included. It is expected that omitting the influence of Poisson's ratio may lead to significant error in practical measurements, especially when the width–thickness ratio of the film is relatively large. In addition, Tarasovs and Andersons [19] and Jiang *et al* [20] assumed that the normal stress on the interface is uniform along the width of the film. However, this is not the case in practice, as will be shown in section 4.3. Quantitative analysis needs to be performed to examine the validity of the assumption of uniform interfacial stress distribution.

In this study, our attention is focused on developing a fundamental solution with higher accuracy for the film-buckling problem. In order to further illustrate the importance of the accuracy of the fundamental solution, we take equation (1) as an example. The elastic modulus of the film from the measured wavelength is determined via the following relation if equation (1) is used:

$$\frac{E_f}{1-\nu_f^2} = \frac{3E_s}{1-\nu_s^2}\left(\frac{\lambda_0}{2\pi h}\right)^3. \tag{2}$$

Equation (2) shows that the measured E_f is sensitive to the errors in the wavelength, λ_0; for instance, an error of 10% in λ_0 will lead to an error of more than 30% in E_f. The errors in the wavelength may originate either from some uncertainties in experiments or from the assumptions made in the derivation of the fundamental relation. Here particular attention is paid to the second aspect in order to develop more accurate and simple relations correlating the buckling wavelength with the film geometry and the material properties of the film and the substrate. To this end, large-scale and fully three-dimensional nonlinear finite element computations are carried out to investigate, under the guideline of dimensional analysis, the buckling of a film with a finite width lying on a compliant substrate. The fundamental relations presented here are very accurate in a broad range of the width–thickness ratio of the film and can be easily used to determine the elastic modulus of the film by the buckling-based measurement method.

2. Dimensional analysis

First, we apply the dimensional analysis method to the buckling problem of a thin film with finite width ideally bonded to a compliant substrate, as shown in figure 1(*a*). The dimensional analysis can provide not only insights into the dependence of the buckling wavelength on the geometry of the film and material properties, but also a guideline for the finite element computations described in the following.

Assume the film/substrate system illustrated in figure 1(*a*) is subjected to an externally applied compressive strain, ε_a, along the length direction of the film. The film may buckle when ε_a exceeds a critical value. Its buckling wavelength, λ, may be a function of the following independent parameters

$$\lambda = f(\varepsilon_a, E_f, \upsilon_f, E_s, \upsilon_s, w, h), \tag{3}$$

where w and h represent the width and thickness of the film, respectively, E is Young's modulus and ν is Poisson's ratio.

This problem involves two-dimensionally independent quantities. Without loss of generality, we take them as E_s and h. The remaining variables are then dimensionally dependent. Consequently, applying the Pi theorem of dimensional analysis [21] to equation (3) gives

$$\lambda = h\Pi\left(\varepsilon_a, \frac{E_f}{E_s}, \upsilon_f, \upsilon_s, \frac{w}{h}\right). \tag{4}$$

For infinitesimal strain problems [2, 20, 22], the dimensionless function Π is independent of ε_a, and equation (4) reduces to

$$\lambda = h\Pi\left(\frac{E_f}{E_s}, \upsilon_f, \upsilon_s, \frac{w}{h}\right). \tag{5}$$

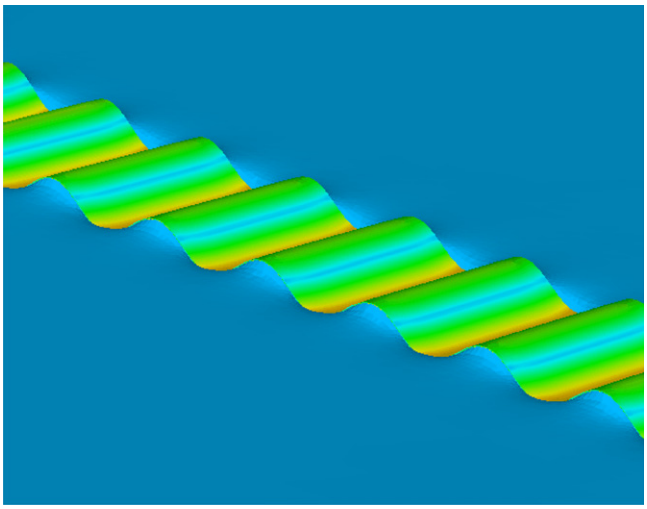

(a)

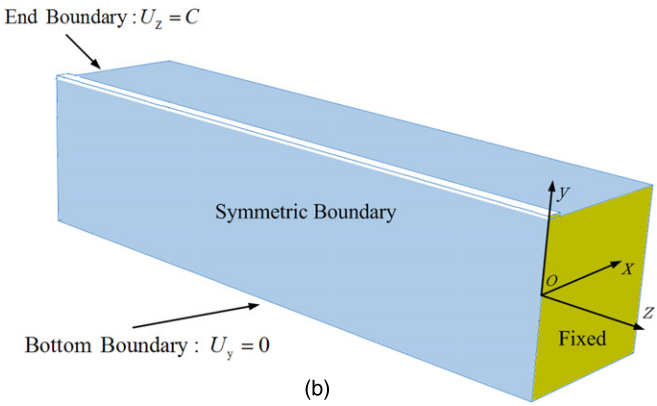

(b)

Figure 1. (*a*) Schematic diagram of a buckled film with a finite width lying on a compliant substrate subjected to compression, (*b*) the boundary conditions applied in the finite element analysis.

For an infinite substrate, introduce the plane-strain modulus as [15, 19, 20, 22]

$$E_s^* = \frac{E_s}{1 - v_s^2}. \tag{6}$$

Then equation (5) is further simplified as

$$\lambda = h\Pi\left(\frac{E_f}{E_s^*}, v_f, \frac{w}{h}\right). \tag{7}$$

For the system in figure 1(*a*), when the film is treated as a plate, the effect of the film's Poisson's ratio will be reflected in the bending stiffness [15, 22, 23]. Thus equation (7) can be re-expressed as

$$\lambda = h\Pi_1\left(\frac{E_f^*}{E_s^*}, \frac{w}{h}\right), \tag{8}$$

where $E_f^* = E_f/(1 - v_f^2)$.

When the film is simplified as a beam [1, 19, 20], the effect of the Poisson's ratio of the film will not come into play and equation (7) reduces to

$$\lambda = h\Pi_2\left(\frac{E_f}{E_s^*}, \frac{w}{h}\right). \tag{9}$$

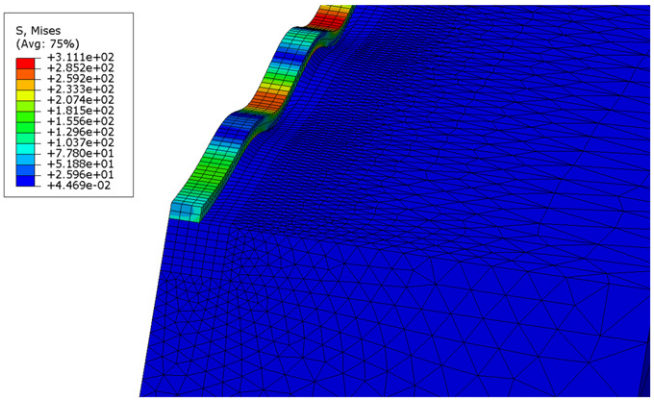

Figure 2. Part of the deformed mesh of finite element model in the computation.

It is expected that the effect of the Poisson's ratio of the film will depend on the ratio w/h. For larger values of w/h, the film may be postulated as a plate while for smaller values of w/h it may be better to treat the film as a beam. In the following section, systematic finite element simulations will be performed to examine the role which the Poisson's ratio plays in the buckling of the film. By supposing the film as a beam, Jiang *et al* [20] recently reported an expression for equation (9). They assumed that the interfacial stress is uniform along the width of the film, which is distinctly different from the actual distribution, as will be shown in section 4.3. Hence, another purpose of our finite element analysis is to examine the error caused by the uniform interfacial stress assumption and to further determine explicit and more accurate expressions of the dimensionless functions Π_1 and Π_2 appearing in equations (8) and (9).

3. Computational model

We performed a large number of three-dimensional finite element computations to study the buckling behaviour of the film/substrate system shown in figure 1(*a*). The computational model for the finite element simulation is schematized in figure 1(*b*). Refer to a Cartesian coordinate system (*o*-*xyz*). The system is symmetric with respect to the *y*–*z* coordinate plane and then, for the sake of simplicity, only a half of the model is simulated in the FEM analysis. The symmetric boundary condition is specified on the symmetric surface. The end of $z = 0$ is fixed and a given displacement is added to the opposite end. The bottom surface is constrained in the *y* direction, and all the other boundaries are traction-free.

Although the strains in the system are small, the problem is geometrically nonlinear and the film undergoes finite rotation. The analysis is carried out by using the commercial finite element software, ABAQUS (Version 6.8.1). The film is perfectly bonded to the substrate using 'tie' constraints in the ABAQUS software. C3D20R element is used for the film, C3D4 and C3D8R elements are used to model the substrate. The modelling system contains nearly 600 000 degrees of freedom. Figure 2 represents the mesh of the computational model.

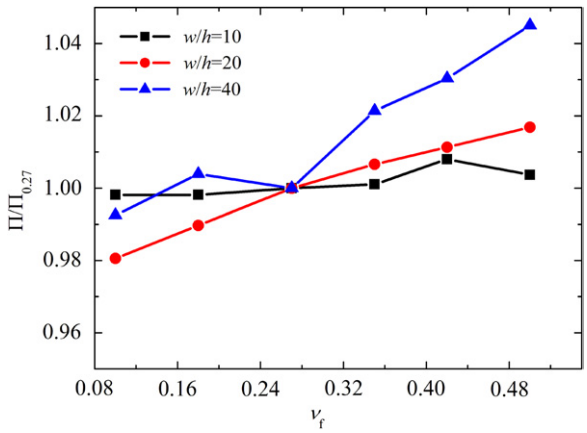

Figure 3. The variation of the normalized dimensionless function Π with respect to the Poisson's ratios of the film. Π is normalized by $\Pi_{0.27}$, which represents the value of Π under $\nu_f = 0.27$.

Convergence analysis is carried out for each given width–thickness ratio w/h of the film. We carefully examine the effects of the substrate dimensions, which are chosen to be sufficiently large (e.g. more than 50 times the film thickness) such that the solutions are insensitive either to the substrate sizes or to the external boundary conditions. In the FEM analysis, the compressive strain is controlled along the z direction such that the assumption of infinitesimal deformation holds.

For each group of geometric and material parameters, only the wavelengths that are homogeneous along the z direction are considered to be effective in data analysis. The wavelengths near to the two ends are ruled out in the analysis due to the boundary effects.

4. Results and discussions

4.1. Effects of the Poisson's ratio of the film on the buckling wavelength

The analysis in section 2 shows that the Poisson's ratio of the film does not come into play when the film is simplified as a beam, and its influence is represented in the plane-strain modulus when the film is modelled as a plate. In this section, we examine the effect of the Poisson's ratio of the film via fully three-dimensional finite element simulations. In the computations, the Young's modulus and Poisson's ratio of the substrate are taken as 10 MPa and 0.45, respectively. The Young's modulus of the film is set as 130 GPa, and its Poisson's ratio varies from 0.1 to 0.5. We take several representative width–thickness ratios of the film, $w/h = 2$, 10, 20, 40 and 100.

For some representative values of the width/thickness ratio w/h and Poisson's ratio ν_f, the normalized dimensionless function Π in equation (7) is calculated and given in figure 3, where $\Pi_{0.27}$ represents the value of Π at $\nu_f = 0.27$. It is seen from the figure that the error in the wavelength λ induced by neglecting the effect of Poisson's ratio ν_f for $w/h = 40$ is around 5%. This could produce an error up to 15% in the measurement of Young's modulus E_f of the film, since E_f is proportional to the cube of λ in the approximate expression in equation (2). Therefore, it may be concluded that only when the ratio w/h is small, it is reasonable to neglect the effect of Poisson's ratio and to treat the film as a beam, as in the theoretical analyses of Jiang *et al* [20] and Tarasovs and Andersons [19]. For larger w/h, figure 3 shows that the effects of ν_f are pronounced, especially for nearly incompressible or incompressible films (e.g. $\nu_f > 0.4$). In this case, it is better to model the film as a plate to account for the effect of ν_f, which can be represented in the plane-strain modulus, as given in equation (8). This point will be further validated in what follows.

4.2. Dependence of the wavelength on the film's geometry and material properties

As described in section 1, the accuracy of the fundamental relation is crucial for determining the film's elastic modulus in the use of the buckling-based measurement method [2] from the viewpoint of inverse analysis. For the buckling of a film with finite width bonded to a compliant substrate, it is difficult to derive an analytical solution correlating the wavelength with the film geometry and material properties. Thus we will determine the explicit expressions of the dimensionless functions Π_1 in equation (8) and Π_2 in equation (9) via systematic finite element computations. In our analysis, the width–thickness ratio of the film, w/h, varies from 2 to 200, and the detailed values of w/h used in the examples are listed in table 1. The Young's modulus of the film varies from 7.5 to 480 GPa, as shown in table 1, while its Poisson's ratio ν_f is kept as 0.27. The Young's modulus and Poisson's ratio of the substrate are fixed as $E_s = 10$ MPa and $\nu_s = 0.45$ in all the examples. The above parameters lead to the variation of E_f^*/E_s^* in the range from 700 to 48 000. More than 100 examples of time-consuming large scale simulations are carried out by using ABAQUS.

Inspired by equation (1) and based on the computational results of the large number of examples, we find that the dimensionless function Π_1 in equation (8) can be given by

$$\Pi_1 = 2\pi \left(\frac{E_f^*}{3E_s^*} \right)^{p_1}, \tag{10}$$

where the exponent p_1 is a function of the width–thickness ratio, w/h. When w is much larger than h, the value of p_1 approaches 1/3 and then the result degenerates to the classical solution given by equation (1). The exponent p_1 is determined by fitting the computational results using equation (10) for the ratio w/h larger than 20. Figure 4 shows the computational results and the curve-fitting results for the ratio $w/h = 40$ and 100, respectively. The exponent p_1 corresponding to different values of w/h is given by the following Prony series (figure 5):

$$p_1 = A_1 e^{[-w/(ht_1)]} + A_2 e^{[-w/(ht_2)]} + A_3 e^{[-w/(ht_3)]} + A_0, \tag{11}$$

where A_0, A_1, A_2, A_3, t_1, t_2 and t_3 are all constants and given in table 2. It is noted that in the determination of Π_1, the Poisson's ratio is taken as $\nu_f = 0.27$ and its effects are represented in the plane-strain modulus. Furthermore, we calculate and compare Π_1 corresponding to different values of Poisson's ratio ν_f in

Table 1. The values of the width/thickness ratio w/h and Young's modulus E_f of the film used in the finite element analysis.

Parameters	Values									
w/h	2	10/3	5	20/3	10	20	200/7	40	100	200
E_f (GPa)	480	340	255	190	130	75	38.5	20	7.5	—

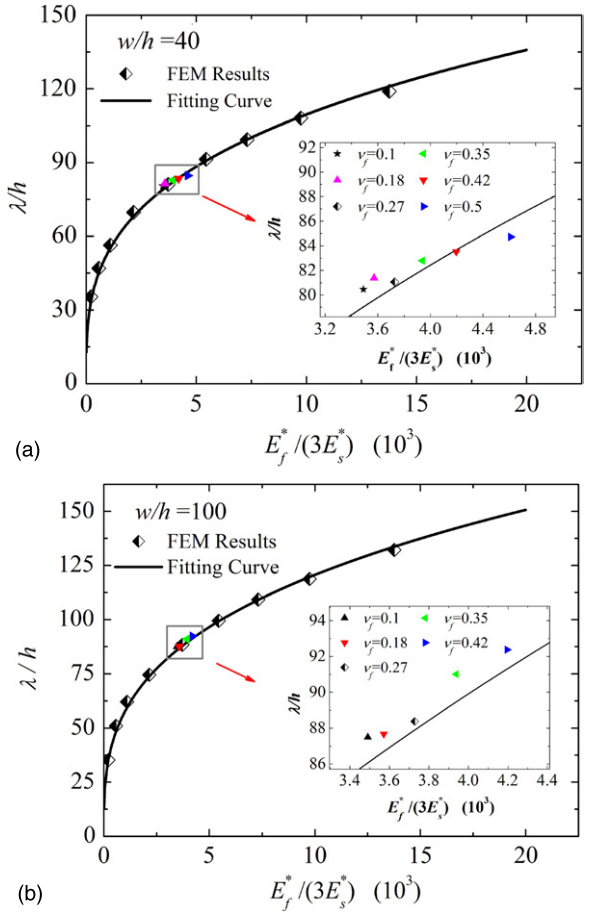

Figure 4. Variation of the normalized wavelength λ/h with respect to the modulus ratio $E_f^*/(3E_s^*)$: (*a*) $w/h = 40$, (*b*) $w/h = 100$, where $E_s^* = E_s/(1-\upsilon_s^2)$ and $E_f^* = E_f/(1-\upsilon_f^2)$.

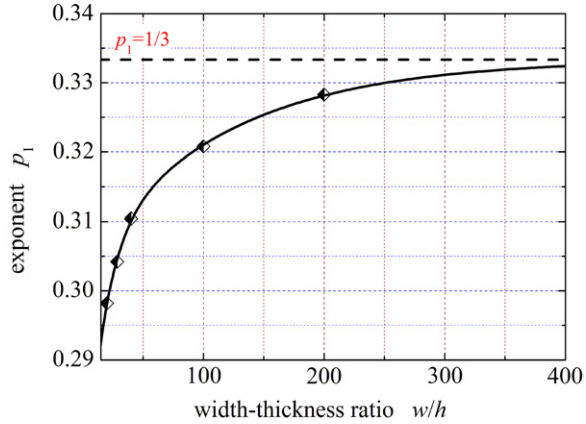

Figure 5. Dependence of the exponent p_1 on the ratio w/h.

the range from 0.1 to 0.5. The results are also given in figure 4 and magnified in the inset. The numerical results match the fitting curve very well, implying that the effect of Poisson's ratio of the film can be well represented by the plane-strain modulus.

According to our above analysis on the effects of the Poisson's ratio of the film, the film can be assumed to be a beam and equation (9) works provided that the ratio w/h is not very large, e.g. $w/h \leqslant 20$. The computational results show that Π_2 can be described by

$$\Pi_2 = 2\pi \left(\frac{E_f}{3E_s^*}\right)^{p_2}. \tag{12}$$

It has a similar form as equation (10) except that the plane-strain modulus E_f^* in equation (10) has been replaced by the elastic modulus of the film E_f in equation (12). The exponent p_2 is also a function of the film's width–thickness ratio, w/h. The dependence relationship of p_2 on w/h is determined by fitting the finite element numerical results using equation (12), as shown in figure 6. The value of p_2 can be well fitted by the following Prony series (figure 7):

$$p_2 = B_1 e^{[-w/(hs_1)]} + B_2 e^{[-w/(hs_2)]} + B_3 e^{[-w/(hs_3)]} + B_0, \tag{13}$$

where B_0, B_1, B_2, B_3, s_1, s_2 and s_3 are all constants and their values are given in table 3. In selecting the fitting functions of p_1 and p_2, the following requirements should be satisfied: (i) they approach 1/3 when w is much larger than h and (ii) the functions fit the numerical results with high accuracy in the whole range of w/h. It is pointed out that fitting functions in other simple forms are also thinkable provided that the above requirements can be satisfied. The difference between equations (10) and (12) lies in the effects of the Poisson's ratio of the film. Figure 3 shows that for a smaller ratio of w/h, the effects of Poisson's ratio υ_f are negligible; however, υ_f begins to influence the buckling wavelength obviously with the increase in w/h. The difference between $\upsilon_f = 0.1$ and $\upsilon_f = 0.5$ comes to about 5% for $w/h = 40$, which will be magnified up to 15% in determining the elastic modulus in the inverse problem. Consequently, significant errors will occur if one applies equation (10) for a smaller ratio of w/h. For a larger ratio of w/h, the effect of υ_f will become remarkable and should be taken into account. Therefore, equation (10) should be employed for wide films while equation (12) is valid for narrow films.

4.3. Validity of the interfacial stress assumption

Based on the theoretical analysis, Jiang *et al* [20] gave a theoretical solution for equation (9) as well as a form of the dimensionless function Π_2. They assumed that the interfacial normal stress σ_y between the film and the substrate is uniform along the width direction of the film. However, figure 8 shows that this is not the case especially when the film width is comparable to its thickness. The magnitude of σ_y

Table 2. Coefficients in equation (11).

Coefficients	A_0	A_1	t_1	A_2	t_2	A_3	t_3
Values	1/3	−0.015 06	116.048 65	−0.042 40	14.652 46	−0.013 96	116.048 20

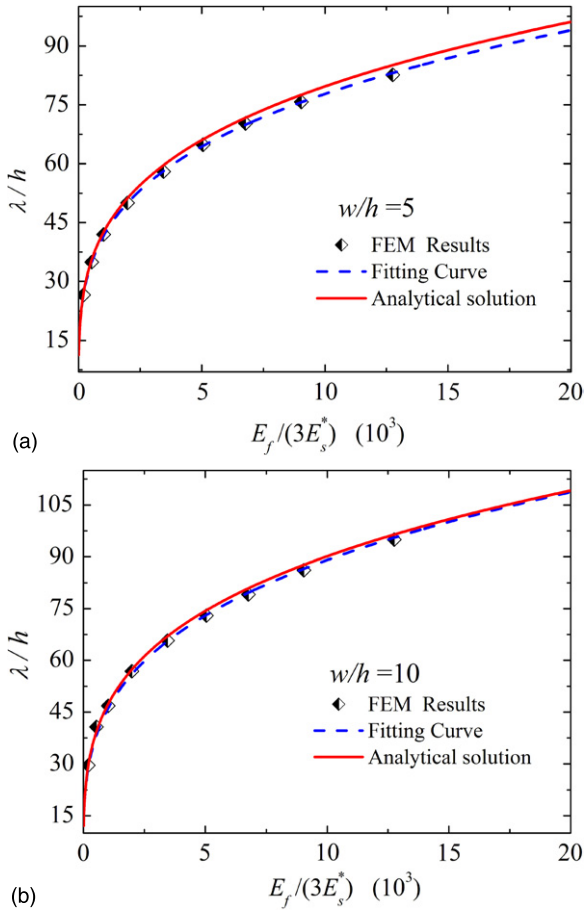

Figure 6. The variation of the normalized wavelength λ/h with respect to the modulus ratio $E_f/(3E_s^*)$, (a) $w/h = 5$; and (b) $w/h = 10$, where $E_s^* = E_s/(1-\upsilon_s^2)$.

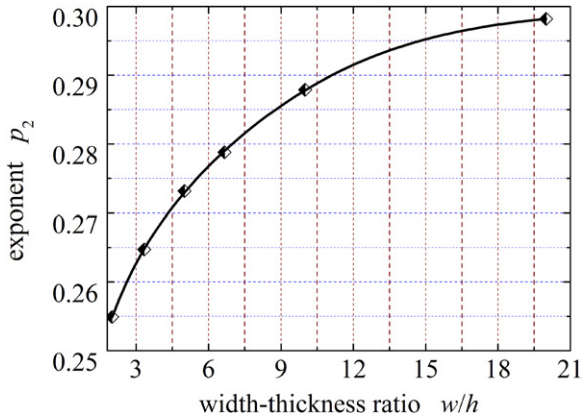

Figure 7. Dependence of the exponent p_2 on the ratio of w/h.

near the edge may have a big difference from that in the middle. Therefore, it is of interest to carefully examine the applicability of the assumption of the uniform interfacial stress σ_y. Our computational results permit us to undertake such a quantitative examination.

The interfacial normal stress along the width is highly nonuniform, as shown in figure 8, especially for a smaller value of w/h. We compare the computational results with the theoretical solution of Jiang *et al* [20]. It is found that under the given material properties and film geometry, the wavelengths predicted by using Jiang *et al*'s solution is in good agreement with the present computational results and the difference is within 5%. Figure 6 gives two typical plots for such a comparison. In figure 6(a), the difference between the numerical and theoretical solutions is less than 3% and in figure 6(b), the difference is smaller than 2%. This indicates that although the actual interfacial stress distribution is not uniform, the uniform assumption in the theoretical analysis is reasonable in most situations.

Considering its good agreements with the computational results, the theoretical solution of Jiang *et al* [20] is still used here to show the applicability of the function form of equation (12). The data points in figure 9 represent the theoretical solution of Jiang *et al* [20] under some typical ratios of w/h and the curves are the numerical fitting results by using equation (12). It is seen that equation (12) can indeed capture the prominent features of the theoretical solution.

5. Conclusions

Using the dimensional analysis and large-scale three-dimensional nonlinear finite element computations of about 200 examples, we studied the buckling of a film with a finite width bonded on a compliant substrate. In summary, the following conclusions have been made.

First, it is shown that the effect of Poisson's ratio depends on the width–thickness ratio of the film. For a smaller ratio of w/h (e.g. $w/h < 20$), this effect is negligible and the fundamental relation can be given by equation (9). For larger ratios of w/h, the Poisson's ratio effect can be represented by the plane-strain modulus and the fundamental relation is formulated in equation (8).

Second, it is demonstrated that the fundamental relations given by equations (8) and (9) can be unified to a simple form, i.e. $\lambda = 2\pi h(r_E)^{p_n}$, where $r_E = E_f^*/(3E_s^*)$ for equation (8) and $r_E = E_f/(3E_s^*)$ for equation (9). The exponent p_n $(n = 1, 2)$ is not a constant but a function of w/h, which has been determined for equations (8) and (9), respectively, by using finite element computations. The results reported here may serve as the fundamental solutions to determine the Young's modulus of the film with a finite width. These relations are convenient and accurate to be used in practical measurements since solving the nonlinear equation is not necessary and a pocket calculator is sufficient.

Additionally, we addressed the effectiveness of the assumption about the interfacial normal stress distribution

Table 3. Coefficients in equation (13).

Coefficients	B_0	B_1	s_1	B_2	s_2	B_3	s_3
Values	0.299 66	1.412 77	2.988 43	−0.718 98	2.543 96	−0.769 26	3.590 32

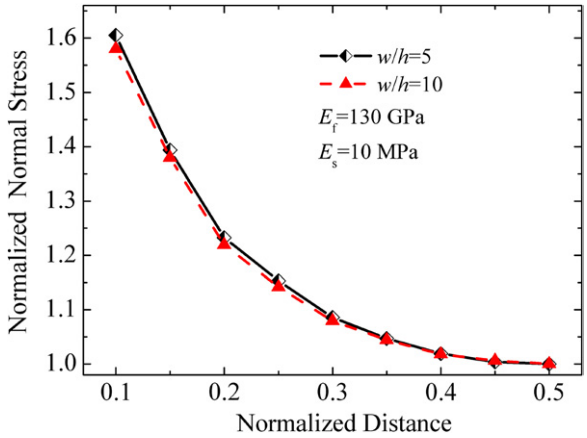

Figure 8. Variation of the normalized normal stress σ_y on the film–substrate interface with the normalized distance from the boundary, where σ_y is normalized by its value at the centre of the film. The distance is measured from the edge of the film to its central line and is normalized by the film width.

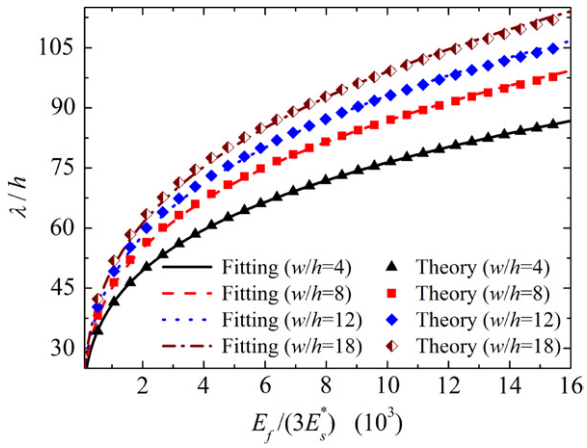

Figure 9. Comparison of the theoretical solution of Jiang *et al* [20] and the fitting results by equation (12) for four representative values of the film's width/thickness ratio, $w/h = 4$, 8, 12 and 18.

made in some recent theoretical analyses. Although the practical interfacial normal stress is not uniform along the width direction of the film, the assumption of the uniform distribution may lead to reasonable results.

Finally, it is worth mentioning that this study is limited to the buckling of a single film with finite width bonded to a soft elastic substrate. In some practical circumstances, multiple strips with finite width on the compliant substrate are used. In recent theoretical work by Jiang *et al*, [20], the buckling of multiple strips with finite width on the elastomeric substrate has been addressed. They concluded that for the wide film, the effect of film spacing is almost negligible, while for narrow thin films, the effect of film spacing is significant. Only when the film spacing reaches about three times the width the effect of film spacing disappears. Further numerical investigation on the interactions among the strips is necessary, which will be considered in the future.

Acknowledgments

The support from the National Natural Science Foundation of China (Grant Nos 10842003, 10525210 and 10732050) and 973 Program (Nos 2004CB619304) is acknowledged.

References

[1] Allen H G 1969 *Analysis and Design of Structural Sandwich Panels* (Oxford: Pergamon) p 157
[2] Stafford C M, Harrison C, Beers K L, Karim A, Amis E J, Vanlandingham M R, Kim H C, Volksen W, Miller R D and Simonyi E E 2004 *Nature Mater.* **3** 545
[3] Stafford C M, Guo S, Harrison C and Chiang M Y 2005 *Rev. Sci. Instrum.* **76** 062207
[4] Stafford C M, Vogt B D, Harrison C, Julthongpiput D and Huang R 2006 *Macromolecules* **39** 5095
[5] Wilder E A, Guo S, Lin-Gibson S, Fasolka M J and Stafford C M 2006 *Macromolecules* **39** 4138
[6] Huang J S, Juszkiewicz M, de Jeu W H, Cerda E, Emrick T, Menon N and Russell T P 2007 *Science* **317** 650
[7] Huang R, Stafford C M and Vogt B D 2007 *ASCE J. Aerospace Eng.* **20** 38
[8] Lacour S P, Wagner S, Huang Z Y and Suo Z 2003 *Appl. Phys. Lett.* **82** 2404
[9] Lacour S P, Jones J, Wagner S, Li T and Suo Z G 2005 *Proc. IEEE* **93** 1459
[10] Khang D Y, Jiang H Q, Huang Y and Rogers J A 2006 *Science* **311** 208
[11] Harrison C, Stafford C M, Zhang W and Karim A 2004 *Appl. Phys. Lett.* **85** 4016
[12] Cerda E and Mahadevan L 2003 *Phys. Rev. Lett.* **90** 074302
[13] Volynskii A L, Bazhenov S, Lebedeva O V and Bakeev N F 2000 *J. Mater. Sci.* **35** 547
[14] Chen X and Hutchinson J W 2004 *J. Appl. Mech.* **71** 597
[15] Huang Z Y, Hong W and Suo Z 2005 *J. Mech. Phys. Solids* **53** 2101
[16] Khang D Y, Xiao J L, Kocabas C, MacLaren S, Banks T, Jiang H Q, Huang Y Y and Rogers J A 2008 *Nano Lett.* **8** 124
[17] Jiang H Q, Khang D Y, Song J Z, Sun Y G, Huang Y G and Rogers J A 2007 *Proc. Natl Acad. Sci. USA* **104** 15607
[18] Song J, Jiang H, Liu Z J, Khang D Y, Huang Y, Rogers J A, Lu C and Koh C G 2008 *Int. J. Solids Struct.* **45** 3107
[19] Tarasovs S and Andersons J 2008 *Int. J. Solids Struct.* **45** 593
[20] Jiang H Q, Khang D Y, Fei H Y, Kim H, Huang Y G, Xiao J L and Rogers J A 2008 *J. Mech. Phys. Solids* **56** 2585
[21] Barenblatt G I 1996 *Scaling, Self-similarity, and Intermediate Asymptotics* (Cambridge: Cambridge University Press) p 7
[22] Groenewold J 2001 *Physica* A **298** 32
[23] Bloom F and Coffin D 2001 *Handbook of Thin Plate Buckling and Postbuckling* (London: Chapman and Hall/CRC press) p 20